Tectonic shortening and coeval volcanism during the Quaternary, Northeast Japan arc

Koji Umeda[1,*], Masao Ban[2], Shintaro Hayashi[3] and Tomohiro Kusano[1]

[1] *Tono Geoscientific Research Unit, Geological Isolation Research and Development Directorate, Japan Atomic Energy Agency, 959-31, Jorinji, Izumi, Toki, 509-5102, Japan.*
[2] *Department of Earth and Environmental Sciences, Yamagata University, 1-4-12 Kojirakawa-machi, Yamagata, 990-8560, Japan.*
[3] *Department of Natural and Environmental Sciences, Akita University, 1-1, Gakuen-machi, Tegata, Akita, 010-8502, Japan.*
[*] *Corresponding author. e-mail: umeda.koji@jaea.go.jp*

The Northeast Japan arc, a mature volcanic arc with a back-arc marginal basin (Japan Sea), is located on a convergent plate boundary along the subducting Pacific plate and the overriding North American plate. From a compilation and analysis of stratigraphy, radiometric age and data on erupted magma volumes, 176 eruptive episodes identified from 69 volcanoes so far, indicate that notable changes in eruption style, magma discharge rates and distribution of eruptive centres occurred around 1.0 Ma. Before ca. 1.0 Ma, large-volume felsic eruptions were dominant, forming large calderas in the frontal arc, a region of low crustal strain rate. After ca. 1.0 Ma to the present, the calc-alkaline andesite magma eruptions in the frontal and rear arcs, synchronous with crustal shortening characterized by reverse faulting, resulted in stratovolcano development along narrow uplifted zones. Although, it is widely assumed that magma cannot rise easily in a compressional setting, some of the magma stored within basal sills could be extruded where N–S-trending uplifted mountains bounded by reverse faults formed since about ca. 1.0 Ma.

1. Introduction

At highly active compressive margins, such as the Northeast (NE) Japan arc, current stresses are mostly compressive and the greatest principal stress is horizontal, indicating that the major faults are thrust faults (e.g., Nakata and Imaizumi 2002). In compressional settings, it is considered that magma cannot ascend easily, favouring magma upwelling along vertical fractures perpendicular to the regional least principal stress (σ_3) (Hubbert and Willis 1957). It has been suggested by many authors that volcanism should be rare if not absent under horizontal compression (e.g., Hamilton 1995; Watanabe *et al.* 1999). However, volcanism is especially common in areas of extensional tectonics, and notably so at divergent plate boundaries (e.g., Galland *et al.* 2007). Similarly, numerous Quaternary volcanoes are distributed in the NE Japan arc, where the Pacific plate is subducting along the Japan Trench under the North American plate at a rate close to the modelled convergence of nearly 9 cm/yr (DeMets 1992). Indeed, the global positioning system measurements reveal large contraction (>0.1 ppm/yr) under compression in the arc (e.g., Sagiya *et al.* 2000). This region is probably one of the most extensively studied volcanic arcs in the world, particularly regarding the relationship

Keywords. Northeast Japan arc; volcanism; tectonic shortening; Quaternary.

between volcanism and tectonics, and high-quality geological, geophysical and geochemical data are readily available (e.g., Hasegawa *et al.* 1978; Zhao *et al.* 1992; Sato 1994; Umeda *et al.* 1999; Yoshida 2001; Tamura *et al.* 2002; Kimura and Yoshida 2006; Acocella *et al.* 2008).

It has recently been recognized that Quaternary volcanoes are clustered in regions trending transverse to their host arc axis, and separated by subparallel, volcano-free gaps 30–75 km wide along the arc (figure 1) (Umeda *et al.* 1999; Tamura *et al.* 2002). The arrangement of the volcanic clusters, coupled with topographic profiles and negative Bouguer anomalies, could be controlled by magma supplied from locally developed hot regions within the mantle wedge (Tamura *et al.* 2002). In the NE Japan arc, a change in the stress field at around the Pliocene to Quaternary boundary resulted in E–W compression (Sato 1994). In connection with the tectonic sequence, felsic volcanism associated with the large calderas terminated and andesite stratovolcanoes became the dominant form of volcanism during the Quaternary (Sato 1994). A compressive stress regime is not favourable to the development of felsic volcanism, requiring the formation of a large magma reservoir at shallow depth (Yoshida 2001). The predominance of stratovolcanoes can be reconciled with the crustal stress field in the present-day subduction system. In contrast, magma discharge rate is inferred to have increased in the NE Japan arc in the late Quaternary. A compilation of age data indicates that volcanoes ranging in age from 2.5 Ma to 1.5 Ma are relatively rare compared with those younger than 1.5 Ma (Kimura and Yoshida 2006). This insight appears to be contradictory to the idea that compressive stress in the Quaternary would prevent the rise of magma within the crust.

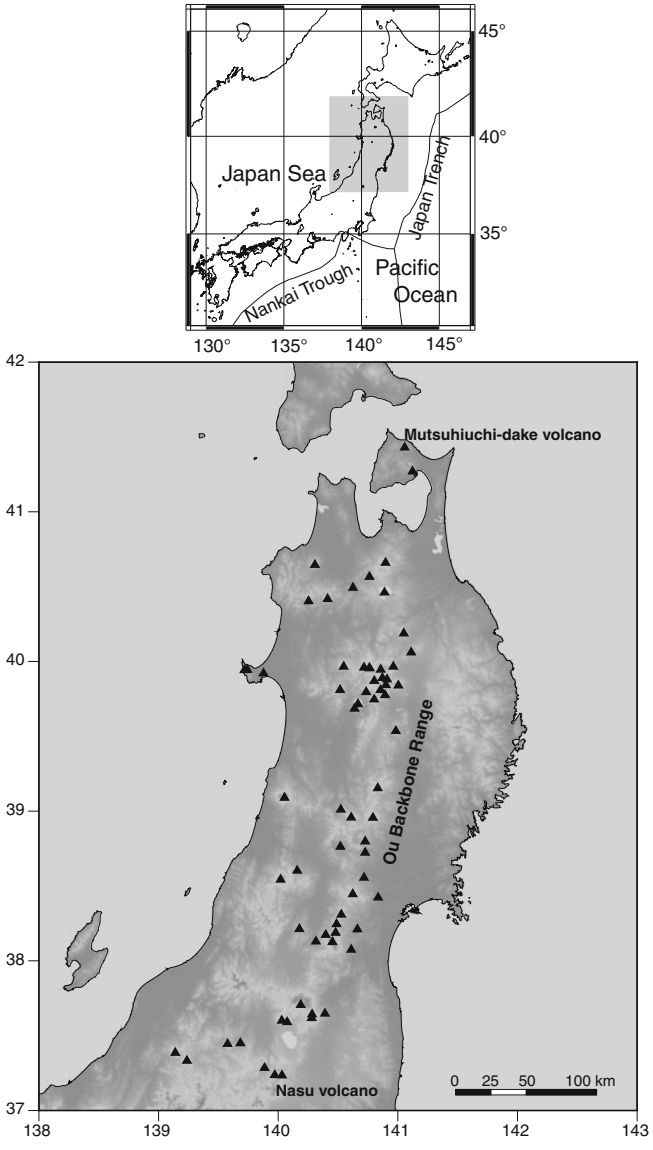

Figure 1. Location and shaded relief maps of NE Japan and distribution of Quaternary volcanoes (black triangles) and active faults (black lines) (Nakata and Imaizumi 2002). Solid triangles and open squares represent stratovolcanoes and large-scale caldera volcanoes, respectively.

Recently, new stratigraphic and radiometric ages of Quaternary volcanoes in the NE Japan arc have been reported, and several synthesized databases were compiled by Umeda *et al.* (1999) and Committee for Catalogue of Quaternary Volcanoes in Japan (1999). Therefore, the special and temporal variations in eruption style, magma discharge rate and distribution of volcanoes during the Quaternary can be recognized with higher resolution than before. With the merging of this type of information, an understanding of the geometric and kinetic features of the structures controlling magma rise and emplacement in convergent settings can be developed. This understanding is also important to applied studies of natural hazards and economic resources. For this paper, we compiled the latest radiometric and stratigraphic data, and calculated the dense-rock equivalent (DRE) (Walker 1980) of volcanic products for each volcano. We describe time–magma volume behaviour that could provide insight into the tectono-magmatic relationships throughout the volcanic arc during the Quaternary. In addition, we examined the mechanism of magma transfer within the crust in a compressional setting.

2. Geological background

The Cenozoic volcanic and tectonic sequence in the NE Japan arc is directly associated with the separation of the present-day NE Japan arc from the Asian continental margin due to the subduction of the Pacific plate and rifting and opening

Table 1. *Ages and magma volume (DRE: dense rock equivalent) for each eruptive episode. Strat., stratigraphical method; TL, thermo-luminescence dating; K–Ar, potassium argon dating;* ^{14}C*, radiocarbon dating; FT, fission track dating. (References for dating: (1) Umeda and Danhara 2008; (2) Arakawa et al. 2008; (3) Suzuki et al. 2005; (4) Committee for Catalog of Quaternary Volcanoes in Japan 1999; (5) Nozawa 2001; (6) Aoki and Arai 2000; (7) Ohba et al. 2003; (8) Kano et al. 2007; (9) Yashima 1990; (10) Fujinawa et al. 2001b; (11) Tsuchiya et al. 1997; (12) Mimura 2001; (13) Mimura and Kano 2000; (14) Umeda et al. 1999; (15) Fujinawa et al. 2001a; (16) Chiba and Kimura 2001; (17) Mimura 2002; (18) Yamamoto 2003, (19) Yamamoto and Komazawa 2004; (20) NEDO 1990).*

Volcano	Eruptive episode	Latitude	Longitude	Age (Ma)	Method	Ref.	DRE (km^3)
Mutsuhiuchi-dake	Older Mutsuhiuchi-dake	41.437	141.057	1.2–0.8	K–Ar	(1)	5.9
Mutsuhiuchi-dake	Younger Mutsuhiuchi-dake	41.437	141.057	0.8–0.5	K–Ar, FT	(1)	3.6
Osorezan	Kamabuse-yama	41.277	141.123	0.80–0.76	K–Ar, FT	(2)	5.6
Osorezan	Byobuyama-Asahinadake	41.277	141.123	0.7–0.5	K–Ar, FT	(2)	3.2
Osorezan	Pre-caldera pyroclastic flow	41.277	141.123	0.48–0.27	K–Ar, FT	(2)	6.4
Osorezan	Post-caldera pyroclastic flow	41.277	141.123	0.27–0.20	K–Ar, FT	(2)	1.3
Osorezan	Tsurugiyama	41.277	141.123	0.2–0.08	K–Ar, FT	(2)	0.1
Hakkoda	Hakkoda P.F. 1st.	40.667	140.897	0.76	Strat.	(3)	17.8
Hakkoda	South-Hakkoda	40.600	140.850	0.65–0.4	K–Ar	(4)	52.4
Hakkoda	Hakkoda P.F. 2nd.	40.667	140.897	0.4	K–Ar	(4)	17.3
Hakkoda	North-Hakkoda	40.650	140.883	0.16–0	K–Ar	(4)	30.4
Iwaki	Iwaki	40.653	140.307	0.330–0.000	K–Ar	(4)	37.2
Okiura	AoniF.Aonigawa P.F.	40.573	140.763	ca. 1.7	K–Ar	(5)	17.6
Okiura	AoniF.Other P.F.	40.573	140.763	1.7–0.9	K–Ar	(5)	3.7
Okiura	Okogawasawalava	40.579	140.759	0.9–0.65	Strat.	(5)	0.9
Okiura	Okiuradacite	40.557	140.755	0.9–0.7	K–Ar	(5)	2.1
Ikarigaseki	Nijikai Tuff	40.500	140.625	ca. 2.0	K–Ar	(4)	20.2
Ikarigaseki	Ajarayama	40.490	140.600	1.91–1.89	K–Ar	(4)	2.1
Towada	Herai-dake	40.450	141.000				5.1
Towada	Ohanabe-yama	40.500	140.883	0.4–0.05	K–Ar	(4)	8.9
Towada	Hakka	40.417	140.867				1.4
Towada	Towada Okuse	40.468	140.888	0.055	^{14}C	(4)	4.8
Towada	Towada Ofudo	40.468	140.888	0.030	Strat.	(6)	22.1
Towada	Towada Hachinohe	40.468	140.888	0.015	Strat.	(6)	26.9
Towada	Post-calderacones	40.457	140.913	0.013–0	Strat.	(4)	14.4
Tashiro	Tashiro	40.425	140.413	0.600–0.470	K–Ar	(4)	6.8
Tashiro	Hirataki P.F.	40.420	140.413	0.020–0.020	Strat.	(4)	0.3
Taira-Komagatake	Taira-Komagatake	40.410	140.254	0.200–0.170	K–Ar	(4)	2.3
Inaniwa	Inaniwa	40.195	141.050	7.000–2.700	K–Ar	(4)	10.6
Nanashigure	Nanashigure	40.068	141.112	1.06–0.72	K–Ar	(4)	55.5
Megata	Megata	39.952	139.742	0.030–0.020	Strat.	(4)	0.0
Toga	Toga	39.950	139.718	ca. 0.42	FT/K–Ar	(4)	1.2
Kampu	Kampu	39.928	139.877	0.030–0.000	Strat.	(4)	0.5
Moriyoshi	Moriyoshi	39.973	140.547	1.07–0.78	K–Ar	(4)	18.1
Bunamori	Bunamori	39.967	140.717	1.2	K–Ar	(4)	0.1
Akita-Yakeyama	Akita-Yakeyama	39.963	140.763	0.5–0	K–Ar	(4)	9.9
Nishimori/Maemori	Nishimori/Maemori	39.973	140.962	0.5–0.3	K–Ar	(4)	2.6
Hachimantai/Chausu	Hachimantai	39.953	140.857	1.0–0.7	K–Ar	(4)	5.5
Hachimantai/Chausu	Chausu-dake	39.948	140.902	0.85–0.75	K–Ar	(4)	13.7
Hachimantai/Chausu	Fukenoyu	39.953	140.857	ca. 0.7	Strat.	(4)	0.2
Hachimantai/Chausu	Gentamri	39.956	140.878		(4)	0.2	
Yasemori/Magarisaki-yama	Magarisaki-yama	39.878	140.803	1.9–1.52	K–Ar	(4)	0.3
Yasemori/Magarisaki-yama	Yasemori	39.883	140.828	1.8	K–Ar	(4)	0.9
Kensomori/Morobidake	Kensomori	39.897	140.871	ca. 0.8	Strat.	(4)	0.8
Kensomori/Morobidake	Morobi-dake	39.919	140.862	1.0–0.8	Strat.	(4)	2.5
Kensomori/Morobidake	1470 m Mt. lava	39.909	140.872	0.72	K–Ar	(7)	0.1
Kensomori/Morobidake	Mokko-dake	39.953	140.857	ca. 1.0	Strat.	(4)	0.5
Tamagawa Welded Tuff	Tamagawa Welded Tuffs R4	39.963	140.763	ca. 2.0	K–Ar	(4)	83.2
Tamagawa Welded Tuff	Tamagawa Welded Tuffs D	39.963	140.763	ca. 1.0	K–Ar	(4)	32.0

Table 1. *(Continued)*

Volcano	Eruptive episode	Latitude	Longitude	Age (Ma)	Method	Ref.	DRE (km^3)
Nakakura/Shimokura	Obuka-dake	39.878	140.883	0.8–0.7	K–Ar	(4)	2.9
Nakakura/Shimokura	Shimokura-yama	39.889	140.933	0.85–0.58	K–Ar	(7)	0.4
Nakakura/Shimokura	Nakakura-yama	39.888	140.910	0.85–0.58	K–Ar	(7)	0.4
Matsukawa	Matsukawa andesite	39.850	140.900	2.6–1.29	K–Ar	(4)	11.6
Iwate/Amihari	Iwate	39.847	141.004	0.2–0	K–Ar	(4)	25.1
Iwate/Amihari	Amihari	39.842	140.958	0.3–0.1	K–Ar	(4)	10.6
Iwate/Amihari	Omatsukura-yama	39.841	140.919	0.7–0.6	K–Ar	(4)	3.3
Iwate/Amihari	Kurikigahara	39.849	140.882				0.2
Iwate/Amihari	Mitsuishi-yama	39.848	140.900	0.46	K–Ar	(4)	0.6
Shizukuishi/Takakura	Marumori	39.775	140.877	0.4–0.3	K–Ar	(4)	2.4
Shizukuishi/Takakura	Shizukuishi-Takakura-yama	39.783	140.893	0.5–0.4	Strat.	(4)	5.2
Shizukuishi/Takakura	Older Kotakakura-yama	39.800	140.900	1.4	K–Ar	(4)	2.7
Shizukuishi/Takakura	North Mikado-yama	39.800	140.875				0.3
Shizukuishi/Takakura	Kotakakura-yama	39.797	140.907	0.6–0.5	K–Ar	(4)	1.8
Shizukuishi/Takakura	Mikado-yama	39.788	140.870	ca. 0.3	Strat.	(4)	0.2
Shizukuishi/Takakura	Tairagakura-yama	39.808	140.878	ca. 0.3	Strat.	(4)	0.1
Nyuto/Zarumori	Tashirotai	39.812	140.827	0.3–0.2	K–Ar	(4)	0.6
Nyuto/Zarumori	Sasamori-yama	39.770	140.820	0.23–0.1	K–Ar	(4)	0.4
Nyuto/Zarumori	Yunomori-yama	39.772	140.827	ca. 0.3		(4)	0.5
Nyuto/Zarumori	Zarumori-yama	39.788	140.850	0.56	K–Ar	(4)	0.9
Nyuto/Zarumori	Nyutozan	39.802	140.843	0.58–0.5	K–Ar	(4)	5.0
Nyuto/Zarumori	Nyuto-kita	39.817	140.855	ca. 0.4	K–Ar	(4)	0.1
Akita-Komagatake	Akita-Komagatake	39.754	140.802	0.1–0	K–Ar	(4)	2.9
Kayo	Kayo	39.803	140.735	2.2–1.17	K–Ar	(4)	5.9
Kayo	KoJiromori	39.828	140.787	0.94	K–Ar	(4)	0.3
Kayo	Akita-Ojiromori	39.839	140.788	1.7	Strat.	(4)	0.3
Daibutsu	Daibutsu	39.817	140.517	2.34–2.16	K–Ar	(4)	2.4
Tazawa	Tazawa	39.723	140.667	1.80–1.40	FT	(8)	
Innai/Takahachi	Takahachi-yama	39.755	140.655	1.7	K–Ar	(4)	0.0
Innai/Takahachi	Innai	39.692	140.638	2.0–1.6	K–Ar	(4)	0.5
Kuzumaru	Aonokimori andesites	39.543	140.983	2.06	K–Ar	(9)	0.3
Yakeishi	Yakeishidake	39.161	140.832	0.7–0.6	K–Ar	(4)	9.5
Yakeishi	Komagatake	39.193	140.924	ca. 1.0	K–Ar	(4)	7.6
Yakeishi	Kyozukayama	39.178	140.892	0.6–0.4	K–Ar	(4)	5.7
Yakeishi	Usagimoriyama	39.239	140.924	0.07–0.04	K–Ar	(4)	2.3
Chokai	Shinsan Lava flow	39.097	140.053	0.02–0	Strat.	(4)	0.6
Chokai	Higashi Chokai	39.097	140.053	0.02–0.02	K–Ar	(4)	3.3
Chokai	Nishi Chokai	39.097	140.020	0.09–0.02	Stra.	(4)	0.6
Chokai	Nishi Chokai II	39.097	140.020	0.13–0.01	K–Ar	(4)	16.0
Chokai	Old Chokai	39.103	140.030	0.55–0.16	K–Ar	(4)	50.9
Chokai	Uguisugawa Basalt	39.103	140.030	0.6–0.55	K–Ar	(4)	0.8
Chokai	Tengumari volcanics	39.103	140.031	0.6–0.55	K–Ar	(4)	8.4
Kobinai	Kobinai	39.018	140.523	1.0–0.57	K–Ar, FT	(4)	2.3
Takamatsu/Kabutoyama	Kabutoyama Welded Tuffs	39.025	140.618	1.16	TL	(4)	3.2
Takamatsu/Kabutoyama	Kiji-yama Welded Tuffs	39.025	140.618	0.30	K–Ar	(4)	5.1
Takamatsu	Takamatsu	38.965	140.610	0.3–0.27	K–Ar	(4)	3.8
Takamatsu	Futsutsuki-dake	38.961	140.661	ca. 0.3		(4)	0.8
Kurikoma	Tsurugi-dake	38.963	140.792	0.1–0	K–Ar	(10)	0.2
Kurikoma	Magusa-dake	38.968	140.751	0.32–0.1	K–Ar	(10)	1.5
Kurikoma	Kurikoma	38.963	140.792	0.4–0.1	K–Ar	(10)	0.9
Kurikoma	South volcanoes	38.852	140.875	ca. 0.5	K–Ar	(10)	0.3
Kurikoma	Older Higashi Kurikoma	38.934	140.779	ca. 0.5	K–Ar	(10)	2.2
Kurikoma	Younger Higashi Kurikoma	38.934	140.779	0.4–0.1	K–Ar	(10)	0.7

Table 1. *(Continued)*

Volcano	Eruptive episode	Latitude	Longitude	Age (Ma)	Method	Ref.	DRE (km^3)
Mukaimachi	Mukaimachi	38.770	140.520	ca. 0.8	K–Ar	(4)	12.0
Onikobe	Shimoyamasato Tuff	38.830	140.695	0.21	FT	(4)	1.0
Onikobe	Onikobe Central cones	38.805	140.727	ca. 0.2	TL	(4)	1.1
Onikobe	Ikezuki Tuff	38.830	140.695	0.3–0.2	FT	(4)	17.3
Naruko	Naruko Central cones	38.730	140.727	0.045	^{14}C	(4)	0.1
Naruko	Yanagizawa Tuff	38.730	140.727	0.045	FT	(4)	4.8
Naruko	Nizaka Tuff	38.730	140.727	0.073	FT	(4)	4.8
Hijiori	Hijiori Pyroclastic flow	38.610	140.159	ca. 0.01	Strat.	(4)	0.5
Hijiori	Komatsubuchi lava dome	38.613	140.171	ca. 0.01	Strat.	(4)	0.0
Gassan	Ubagatake	38.533	140.005	0.400–0.300	K–Ar	(4)	2.7
Gassan	Yudonosanlavas/pyroclastics	38.534	139.988	0.800–0.700	K–Ar	(4)	5.7
Gassan	Gassan	38.550	140.020	0.500–0.400	K–Ar	(4)	13.7
Funagata	Izumigatake	38.408	140.712	1.45–1.14	K–Ar	(4)	2.3
Funagata	Funagatayama	38.453	140.623	0.85–0.56	K–Ar	(4)	19.0
Yakuraisan	Yakuraisan	38.563	140.717	1.65–1.04	K–Ar	(11)	0.2
Nanatsumori	Nanatsumori lava	38.430	140.835	2.3–2.0	K–Ar	(12)	0.5
Nanatsumori	Miyatoko Tuffs	38.428	140.793	ca. 2.5	Strat.	(4)	6.1
Nanatsumori	Akakuzure-yama lava	38.433	140.768	1.6–1.5	Strat.	(4)	1.5
Nanatsumori	Kamikadajin lava	38.447	140.772	1.6–1.5	K–Ar	(4)	0.8
Shirataka	Shirataka	38.220	140.177	1.0–0.8	K–Ar	(13)	3.8
Adachi	Adachi	38.218	140.662	0.08	FT	(4)	0.9
Gantosan	Gantosan	38.195	140.480	0.4–0.3	K–Ar	(4)	4.6
Kamuro-dake	Kamuro-dake	38.253	140.488	1.67	K–Ar	(12)	5.7
Daito-dake	Daito-dake	38.316	140.527	ca. 1.0	Strat.	(4)	5.7
Sankichi-Hayama	Sankichi-Hayama	38.137	140.315	2.400–2.300	K–Ar	(4)	2.2
Ryuzan	Ryuzan	38.181	140.397	1.1–0.9	K–Ar	(4)	4.6
Zao	Central Zao 1st.	38.133	140.453	1.46–0.79	K–Ar	(14)	0.8
Zao	Central Zao 2nd.	38.133	140.453	0.32–0.12	K–Ar	(14)	15.2
Zao	Central Zao 3rd.	38.133	140.453	0.03–0	K–Ar	(14)	0.0
Zao	Sugigamine	38.103	140.462	1.0	K–Ar	(14)	9.9
Zao	Fubosan/byobudake	38.093	140.478	0.31–0.17	K–Ar	(14)	15.2
Aoso-yama	Gairinzan	38.082	140.610	0.7–0.4	K–Ar	(12)	6.1
Aoso-yama	Central Cone	38.082	140.610	0.40–0.3	K–Ar	(4)	3.0
Azuma	Azuma Kiteilava	37.733	140.247	1.3–1.0	K–Ar	(4)	24.7
Azuma	Higashi Azumasan	37.710	140.233	0.7–0	K–Ar	(4)	22.8
Azuma	Nishi Azumasan	37.730	140.150	0.6–0.4	K–Ar	(4)	7.2
Azuma	Naka Azumasan	37.713	140.188	0.4–0.3	K–Ar	(4)	4.6
Nishikarasugawaandesite	Nishikarasugawa andesite	37.650	140.283	ca. 1.5	K–Ar	(4)	1.9
Adatara	Adatara Stage 1	37.625	140.280	0.55–0.44	K–Ar	(15)	0.3
Adatara	Adatara Stage 2	37.625	140.280	ca. 0.35	K–Ar	(15)	0.4
Adatara	Adatara Stage 3a	37.625	140.280	ca. 0.20	K–Ar	(15)	2.0
Adatara	Adatara Stage 3b	37.625	140.280	0.12–0.002	K–Ar	(15)	0.3
Sasamori-yama	Sasamari-yama andesite	37.655	140.391	2.5–2	K–Ar	(4)	0.4
Bandai	Pre-Bandai	37.598	140.075	ca. 0.7	K–Ar	(4)	0.1
Bandai	Bandai	37.598	140.075	0.3–0	Strat.	(16)	14.0
Nekoma	Old Nekoma	37.608	140.030	1.0–0.7	K–Ar	(17)	11.4
Nekoma	New Nekoma	37.608	140.030	0.5–0.4	K–Ar	(17)	0.9
Numazawa	Shirifukitoge P.	37.452	139.577	0.11	FT	(18)	0.7
Numazawa	Mukuresawa L.	37.452	139.577	0.071	TL	(18)	0.1
Numazawa	Mizunuma P.	37.452	139.577	0.045	^{14}C	(18)	1.0
Numazawa	Sozan L.	37.452	139.577	0.043	FT	(18)	0.3
Numazawa	Numagozen P.	37.452	139.577	0.0198	^{14}C	(18)	0.0
Numazawa	Maeyama L.	37.452	139.577	0.02	^{14}C	(18)	0.3

Table 1. *(Continued)*

Volcano	Eruptive episode	Latitude	Longitude	Age (Ma)	Method	Ref.	DRE (km^3)
Numazawa	Numazawako P.	37.452	139.577	0.005	^{14}C	(18)	2.0
Sunagohara	Sunagohara	37.457	139.684	0.29–0.22	FT	(19)	2.7
Sumon	Sumon	37.393	139.140	2.40–1.75	K–Ar	(4)	22.0
Asakusa	Asakusa	37.340	139.237	1.64–1.54	K–Ar	(4)	4.6
Kasshi/Oshiromori	Kasshi	37.184	139.973				0.1
Kasshi/Oshiromori	Oshiromori	37.199	139.970				0.7
Kasshi/Oshiromori	Matami-yama	37.292	139.886	0.94	K–Ar	(20)	0.3
Kasshi/Oshiromori	Naka-yama	37.282	139.899				0.0
Shirakawa	Kumado P.F.	37.242	140.032	1.31	K–Ar	(4)	19.2
Shirakawa	Tokaichi A.F. tuffs	37.242	140.032	1.31–1.24	Strat.	(4)	12.0
Shirakawa	Ashino P.F.	37.242	140.032	1.2	FT	(4)	19.2
Shirakawa	Nn3 P.F.	37.242	140.032	1.20–1.17	Strat.	(4)	0.0
Shirakawa	Kinshoji A.F. tuffs	37.242	140.032	1.20–1.18	Strat.	(4)	9.0
Shirakawa	Nishigo P.F.	37.252	139.869	1.11	FT	(4)	28.8
Shirakawa	Tenei P.F.	37.242	140.032	1.06	Strat.	(4)	7.7
Nasu	Futamata-yama	37.244	139.971	0.14	K–Ar	(4)	3.2
Nasu	Kasshiasahi-dake	37.177	139.963	0.6–0.4	K–Ar	(4)	12.3
Nasu	Sanbonyari-dake	37.147	139.965	0.4–0.25	K–Ar	(4)	5.5
Nasu	Minamigassan	37.123	139.967	0.2–0.05	K–Ar	(4)	8.7
Nasu	Asahi-dake	37.134	139.971	0.2–0.05	K–Ar	(4)	4.6
Nasu	Chausu-dake	37.122	139.966	0.04–0	K–Ar	(4)	0.3

of the Japan Sea. The main rifting started at ~23 Ma (Taira 2001). Between 21 and 18 Ma, rifting was accompanied by significant counter-clockwise rotation of the NE Japan arc (Jolivet *et al.* 1994). Owing to the cessation of the opening of the Japan Sea, the extensional stress field changed at about 13 Ma. From the Middle Miocene to the Pliocene, the tectonics is characterized by very weak crustal deformation under the moderate regional stress field related to the convergence of the Pacific plate (Sato 1994). The maximum horizontal stress oriented in the NE or ENE direction was manifested during this period. This is one of the reasons why the SW migration of the Kuril sliver due to the oblique convergence along the Kuril arc results from a NE or ENE trending maximum compression (e.g., Otsuki 1990). In relation to the stress change from extensional to a slightly compressive stress, a major variation in the volcanism in the NE Japan arc changed from rift-type into island-arc type in the last 13 Ma (Sato 1994; Yoshida 2001), resulting in changes in the location and orientation of the volcanic front (Ohguchi *et al.* 1989). Submarine basaltic to rhyolitic volcanism was predominant from 13 to 8 Ma. Many Valles-type caldera (volcanic crater formed by collapse during an ignimbrite eruption) formed on the central mountains range along the arc since ca. 8 Ma. The dome-like structures around the calderas indicate that felsic magmatism in the shallow crust contributed to the gentle uplift of the central mountains range (Yoshida 2001).

Tectonic shortening of the crust due to E–W compression became apparent at about the Pliocene to Quaternary boundary, which may be associated with the increased motion of the Pacific Plate between 5 and 2 Ma (Cox and Engebretson 1985; Pollitz 1986). A compressional stress field during the Quaternary is responsible for the development of two narrow uplift zones oriented in a N–S direction, in the NE Japan arc: the Ou Backbone Range (fore-arc) and the Dewa Hills (rear-arc). They appear to be an active pop-up structure bounded by opposite-facing reverse faults accommodating <5 mm/yr of E–W shortening across the range (Hasegawa *et al.* 2005). Based on the subsurface geology and deformation of river terraces, the initiation time of reverse faulting was estimated at several sites in the NE Japan. These results suggest that reverse faulting started on the rear-arc side between 3.4 and 2.4 Ma (Awata and Kakimi 1985), and in the fore-arc side between 0.9 and 0.5 Ma (Otsuki *et al.* 1977), corresponding to the onset time of uplift of the Dewa Hills and the Ou Backbone Range. The compressional regime reactivated originally normal faults related to the extensional back-arc rifting as reverse faults and these accommodate much of the ongoing shortening across the arc. Andesite stratovolcanoes started to form between 2.5 and 1.5 Ma, but these are

relatively rare compared with those younger 1.5 Ma volcanoes (Kimura and Yoshida 2006). Nevertheless, it remains obscure as to when the calc-alkaline andesite volcanism, derived from the mixing between the felsic and mafic magmas (e.g., Sakuyama and Nesbitt 1986), has been established under Quaternary orthogonal convergence in the NE Japan arc.

3. Estimation of timing and volume for each eruptive episode

Although 34 Quaternary volcanoes have been recognized along the volcanic arc between Mutsuhiuchi-dake volcano and Nasu volcano in the NE Japan arc (Ono *et al.* 1981), they are predominantly polygenic, with new edifices forming at new locations and evolving into polygenic volcano centres. Before refining the sequence of volcanism during the Quaternary, we subdivided individual volcanoes identified by Ono *et al.* (1981) into as small a units as possible. The term 'eruptive episode' used herein refers to any unit that formed due to a series of eruptions from the same conduit or edifice, including monogenic volcanoes (volcano constructed during a single phase of eruptive activities) that formed in a relatively short time period and polygenetic volcanoes (resulting in from more than one formation process) that developed over several tens to hundreds of thousands of years. The active time span of eruptive episode with several radiometric ages can be estimated by their median age. Radiometric ages that are inconsistent with the stratigraphic data were discarded.

The magma volume discharged for each eruptive episode was calculated as follows: Assuming that a edifice is represented by a cone with a radius of basal circle (R) and height between the base and apex (H), volume (V) is calculated by the following equation: $V = (1/3)\,H\pi R^2$. When it is represented by an elliptical cone, the radius of a basal circle (R') with the same area as the basal ellipse is found, and then the R' is applied in the above equation (Umeda *et al.* 1999). The relief of the underlying basement can be considered. For example, when the basement of the conical edifice is uplifted in the central part to form a raised bottom, the excessive volume is subtracted from the conical volume. The volume of lava flows or pyroclastic flows is calculated by multiplying their basal area and average thickness. When it is difficult to estimate the average thickness, their distribution area is subdivided into smaller areas by taking into account basement relief, and the products of their area and average thickness in the respective subdivided areas are totalled. The DRE of erupted volumes was calculated by the product of volume and density of the respective volcanic products. Density values used are: stratovolcanoes, 1.9 g/cm^3; non-welded pyroclastic flow deposits, 1.2 g/cm^3; welded pyroclastic flow deposits, 1.6 g/cm^3; pyroclastic fall deposits, 1.5 g/cm^3 (Nakamura 1964; Smith 1979; Yoshida and Takahashi 1991).

Table 1 presents the locations, active time spans (range), and magma volumes of the individual eruptive episodes during the Quaternary, including the Gelasian Stage. Sixty-nine volcanoes composed of 176 eruptive episodes can be identified along the volcanic arc between Mutsuhiuchi-dake volcano and Nasu volcano (figure 1).

4. Time–volume relationships for NE Japan volcanic arc since 2.0 Ma

In order to elucidate temporal variations in the long-term magma discharge rate for all of the NE Japan

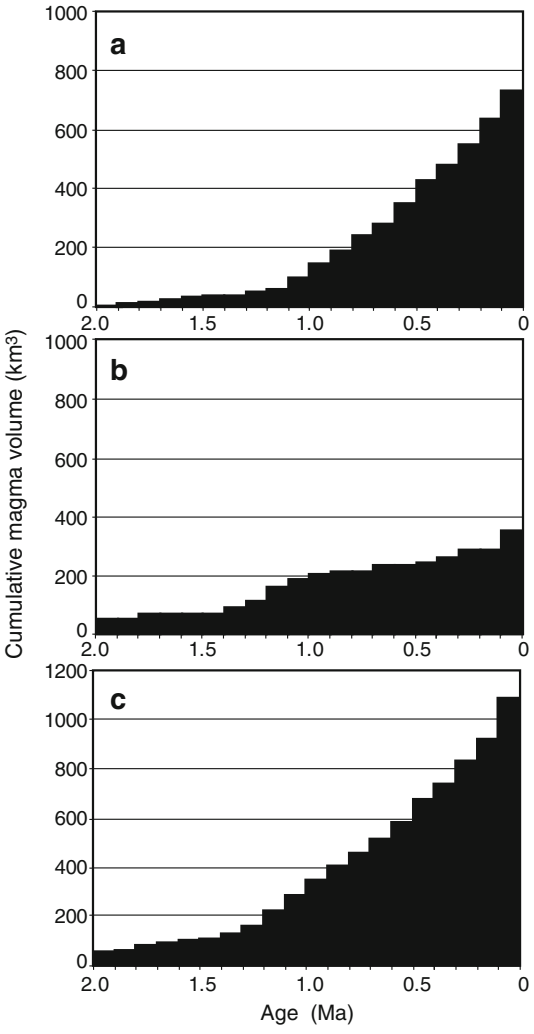

Figure 2. Time–volume relationships for the NE Japan volcanic arc since 2.0 Ma. (**a**) Volcanism associated with stratovolcanoes, (**b**) felsic volcanism associated with the large calderas, and (**c**) total erupted magma volume.

arc, the magma volume erupted every 100,000-year period (long-term discharge rate of magma) was calculated for each volcano since 2.0 Ma. In the case of South-Hakkoda eruptive episode between 0.65 and 0.40 Ma belonging to Hakkoda volcano (table 1), the erupted volume was estimated to be 52.4 km^3 magma from which 10.4, 21.0 and 21.0 km^3 magmas can be allocated to the periods of 0.7–0.6, 0.6–0.5 and 0.5–0.4 Ma, respectively.

Figure 2 shows plots of cumulative volume associated with large, felsic calderas and andesitic stratovolcanoes as a function of their ages. It indicates that eruptive volume flux of andesitic stratovolcanoes increased significantly after 1.1 Ma. Although flux of eruptive volume from large, felsic calderas increase slightly between 1.4 and 1.0 Ma, the slope, except the slightly anomalous period indicates a constant flux of ∼0.1 km^3/ky. Accordingly, volcanism can be divided into two stages: Stage 1 (before ca. 1.0 Ma) is characterized by the predominance of large-volume felsic eruptions forming large calderas, Stage 2 (ca. 1.0 Ma onwards), is dominated by calc-alkaline andesite stratovolcano-building eruption, except for Towada volcano. Stage 2 is marked by a significant increased magmatism in the entire NE Japan arc. Felsic volcanism, dominant in Stage 1, is believed to have occurred under neutral to weak compressional stress fields associated with gentle uplifting of volcanic arc (Yoshida 2001).

There are two fundamental types of time–volume relationships for volcanic fields: volume-predictable behaviour (linear relationship between the cumulative volume of an eruptive episode plus prior episodes and its timing) and time-predictable behaviour (linear relationship between the timing of an episode and the cumulative volume of prior episodes only). A plot of total volume–age relationship throughout the NE Japan arc suggests that it appears to change somewhat from the time-predictable trend into the volume-predictable trend around 1.0 Ma (figure 2). Valentine and Perry (2007) suggested that eruption marked by the volume-predictable trend occurs in magmatically controlled fields (high magma fluxes), where pressures build up in magma reservoirs, driven primarily by process such as melt accumulation, fractionation, and concentration of volatiles.

Most of the volcanoes exist on uplifted regions forming a topographic high known as the Ou Backbone Range. In addition, E–W volcanic zones have been developed with several volcanoes in the rear arc (figure 1). It should be noted that the distribution of volcanoes formed in Stage 1 is limited on the Ou Backbone Range. However, Stage 2 is characterized by volcanism extended to the rear arc, suggesting that Quaternary NE Japan volcanism, stratovolcanoes arranging in E–W direction perpendicular to the volcanic arc, have been established since ca. 1.0 Ma (figure 3).

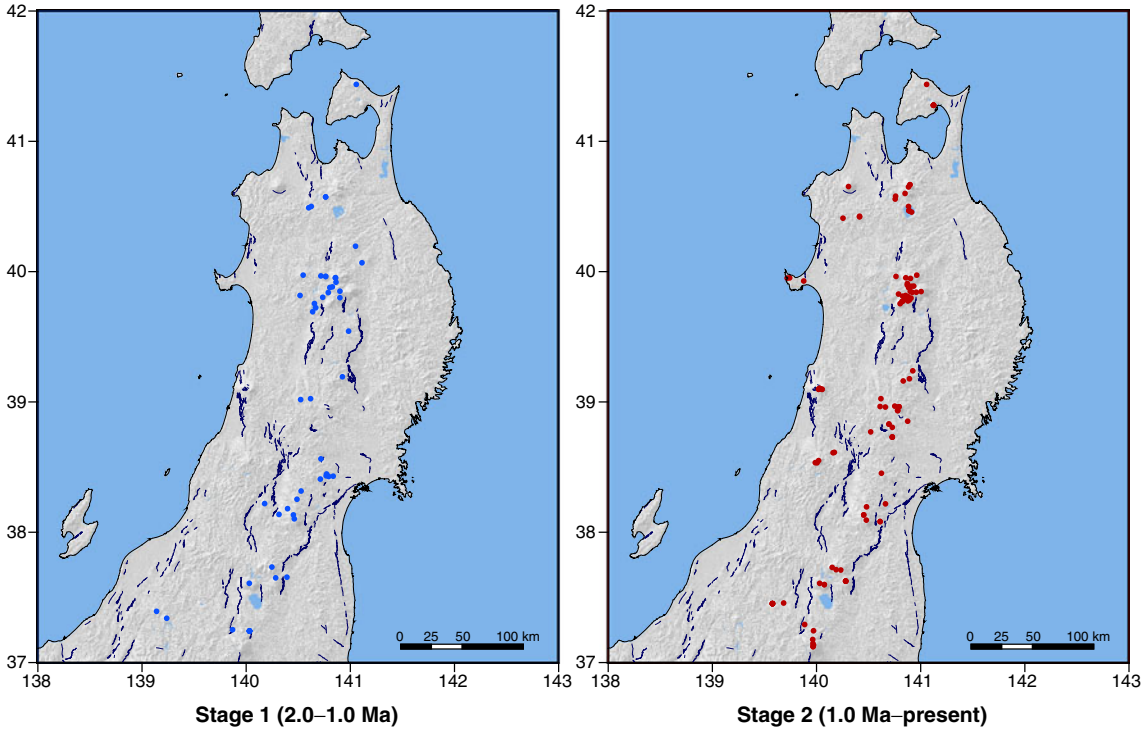

Figure 3. Distribution of eruptive centres for Stage 1 (2.0–1.0 Ma) and Stage 2 (1.0–0 Ma). Also shown in this figure are active faults.

5. Discussion and conclusions

As mentioned in the previous section, the NE Japan arc has been undergoing E–W compression without any significant oblique component during the Quaternary, and reverse faulting has occurred across the entire volcanic arc since about 1.0 Ma, resulting in the predominance of the N–S trending thrusts with crustal shortening. Contemporaneous changes in volcanism occurred as well; around 1.0 Ma, andesite volcanism with stratovolcano-forming eruptions was initiated. Moreover, magma discharge rate in the entire volcanic arc has rapidly increased since ca. 1.0 Ma. At the same time, the magma underwent a systematic change in chemical composition. A significant volume of medium-K andesite has been erupted along the Ou Backbone Range since 1.0 Ma to 0.7 Ma, together with subordinate low-K andesite (Ban *et al.* 1992). What are the processes linked to volcanic and tectonic changes around 1.0 Ma in the NE Japan arc? Several researchers insist that the Pacific plate underwent significant changes in the amount and absolute direction of motion between 5 and 2 Ma (Cox and Engebretson 1985; Pollitz 1986). These studies agree on a significant increase in the subduction rate of the Pacific plate, estimated, in the NE Pacific, between ∼30 and ∼70%. In consequence, the NE Japan arc has been undergoing active compressional inversion with shortening intensifying over 2.0 Ma.

However, despite compressional stress regime ($\sigma_v = \sigma_3 < \sigma_2 < \sigma_1$), a large amount of magma has been extruded since ca. 1.0 Ma. One of the plausible explanations for this contradiction may be the increase in magma generation in the mantle wedge. Numerical simulations considering fluid migration and melting in the mantle wedge above a subducting plate indicate that melt production rates increase with increasing convergence rate (Cagnioncle *et al.* 2007). In the Cascade volcanic arc, the convergence rate of the Juan de Fuca plate to the North American plate is thought to control the change in eruption rate (Priest 1990). Therefore, despite the overall compressive setting along the NE Japan arc, the increase in volume of magma could be due to the increase in degree of partial melting in the mantle wedge promoted by significantly faster subducting Pacific plate.

In addition, recent experimental modelling provided insight into the upwelling process of magma within brittle crust under a compressive stress regime (Galland *et al.* 2007). These researchers employed (1) silica powder to replicate a brittle crust and (2) liquid vegetable oil representing magma, to model materials. Under compressional settings using a steadily advancing piston, the silica powder 'crust' shortened as the result of the thrust fault development, which had straight traces at the free surface. When shortening of the silica powder and injection of the oil were simultaneous, magma formed a basal sill and then typically rose along a thrust fault. These results imply that, theoretically, compression favours the emplacement of sills (Hubbert and Willis 1957), but thrust faults then provide vertical tension fractures serving as conduits for magma in the shallow portion of the hanging wall, demonstrating that magma can propagate to the Earth's surface in a tectonic regime characterized by contracting deformation. These structures can be attributed to superposition of a local load, due to the uplifted zone, on the regional stress field (Molnar 1986). Therefore, apparent thrust faulting throughout the Ou Backbone Range since ca. 1.0 Ma could facilitate the effective transfer of magma from the crust and localize newly formed volcanoes close to thrust faults on Ou Backbone Range.

Consequently, volcanism associated with andesite stratovolcanoes, and thrust faulting due to tectonic shortening has been clearly active since ca. 1.0 Ma, in the NE Japan arc. This is because the increased melt production rate within the mantle wedge and compressional stress regime is ascribed to a significant increase in the subduction rate of the Pacific plate between 5 and 2 Ma. The contractional tectonic settings that form a basal sill for magma prevent magma from reaching the Earth's surface. Nevertheless, some volume of magma from the basal sill could be extruded onto the surface where uplifted mountains, bounded by reverse faults, perpendicular to the volcanic arc, have been established since ca. 1.0 Ma. Rather slow ascent of magma from the basal sill may allow differentiated felsic magma within the upper crust to mix with primary magma arising from the deeper potion, such as lower crust and/or mantle wedge, resulting in the production of calc-alkaline andesite volcanism.

Acknowledgements

The authors would like to thank T Ohba, M Sasaki and K Akaishi for helpful discussions. Careful reviewing of R I Tilling, S J Day, G F McCrank and the anonymous reviewers has greatly improved the paper.

References

Acocella V, Yoshida T, Yamada R and Funiciello F 2008 Structural control on Late Miocene to Quaternary volcanism in the NE Honshu arc, Japan; *Tectonics* **27** TC5008, doi: 10.1029/2008TC002296.

Aoki K and Arai F 2000 Late Quaternary tephrostratigraphy of Marine Core KH94-3, LM-8 off Sanriku, Japan; *Quat. Res.* **39** 107–120.

Arakawa T, Okajima T, Mizukami K, Shimura S, Miyawaki R, Momose M, Kobayashi M and Yoshida M 2008 Eruption history on Osore-zan Volcano, Shimokita peninsula: Long-term change of magma eruptive rate and eruption style, etc; *Abst. Volcanol. Soc. Japan 2008 Fall Meeting* A16.

Awata Y and Kakimi T 1985 Quaternary tectonics and damaging earthquakes in northeast Honshu, Japan; *Earthq. Predict. Res.* **3** 231–251.

Ban M, Oba Y, Ishikawa K and Takaoka N 1992 K–Ar dating of Mutsu-Hiuchidake, Osoreyama, Nanashigure, and Aoso volcanoes of the Aoso-Osore volcanic zone – The formation of the present volcanic zonation of the Northeast Japan arc; *J. Mineral. Petrol. Econ. Geol.* **87** 39–49.

Cagnioncle A-M, Parmentier E M and Elkins-Tanton L T 2007 Effect of solid flow above a subducting slab on water distribution and melting at convergent plate boundaries; *J. Geophys. Res.* **112** B09402, doi: 10.1029/2007JB004934.

Chiba S and Kimura J 2001 Geology and growth history of Bandai volcano, Tohoku-Honshu arc, Japan: Analysis of volcanic activity by tephrochronology; *Japan Mag. Mineral. Petrol. Sci.* **30** 126–156.

Committee for Catalogue of Quaternary Volcanoes in Japan 1999 *Catalogue of Quaternary Volcanoes in Japan* (Tokyo: Volcanology Society of Japan).

Cox A and Engebretson D 1985 Change in motion of Pacific Plate at 5 Myr BP; *Nature* **313** 472–475.

DeMets C 1992 Oblique convergence and deformation along the Kuril and Japan trenches; *J. Geophys. Res.* **97** (B12) 17615–17625.

Fujinawa A, Hayashi S and Umeda K 2001a K–Ar ages for lava samples of Adatara volcano: Reexamination of formation history of the volcano; *Bull. Volcanol. Soc. Japan* **46** 95–106.

Fujinawa A, Fujita K, Takahashi M, Umeda K and Hayashi S 2001b Development history of Kurikoma volcano, Northeast Japan; *Bull. Volcanol. Soc. Japan* **46** 269–284.

Galland O, Cobbold P R, de Bremond d'Ars J and Hallot E 2007 Rise and emplacement of magma during horizontal shortening of the brittle crust: Insights from experimental modeling; *J. Geophys. Res.* **112** B06402, doi: 10.1029/2006JB004604.

Hamilton W B 1995 Subduction systems and magmatism; In: *Volcanism Associated with Extension at Consuming Plate Margins* (ed.) Smellie J L, *Geol. Soc. London, Spec. Publ.* **81** 3–28.

Hasegawa A, Umino N and Takagi A 1978 Double-planed structure of the deep seismic zone in the northeastern Japan arc; *Tectonophys.* **47** 43–58.

Hasegawa A, Nakajima J, Umino N and Miura S 2005 Deep structure of the northeastern Japan arc and its implications for crustal deformation and shallow seismic activity; *Tectonophys.* **403** 59–75.

Hubbert M K and Willis D G 1957 Mechanics of hydraulic fracturing; In: *Structural geology* (ed.) Hubbert M K (New York: Hafner Publishing Company), pp. 175–190.

Kano K, Ohguchi T, Hayashi S and Yanai K 2007 Tazawako caldera and its eruption products; *Abst. Geol. Soc. Japan 114th Annual Meeting* O–17.

Jolivet L, Tamaki K and Fournier M 1994 Japan Sea, opening history and mechanism: A synthesis; *J. Geophys. Res.* **99(B11)** 22,237–22,259.

Kimura J and Yoshida T 2006 Contribution of slab fluid, mantle wedge and crust to the origin of Quaternary lavas in the NE Japan Arc; *J. Petrol.* **47** 2185–2232.

Mimura K 2001 K–Ar dating of Nanatsumori volcanic rock, Kamurodake and Aoso volcanoes along the Quaternary volcanic front of northeast Japan; *Bull. Volcanol. Soc. Japan* **52** 309–313.

Mimura K 2002 Geology and radiometric ages of Nekoma Volcano, Northeast Japan; *Bull. Volcanol. Soc. Japan* **47** 217–225.

Mimura K and Kano K 2000 Stratigraphy and history of Shirataka Volcano, NE Japan; *Bull. Volcanol. Soc. Japan* **45** 13–23.

Molnar P 1986 The structure of mountain ranges; *Sci. Amer.* **255** 64–73.

Nakamura K 1964 Volcano-stratigraphic study of Oshima volcano, Izu; *Bull. Earthq. Res. Inst.* **42** 649–728.

Nakata T and Imaizumi T 2002 *Digital active fault map of Japan (DVD-ROM)* (Tokyo: University of Tokyo Press), p. 60.

NEDO 1990 *Explanatory text of the volcano-geological map and compiled geological map of Nasu geothermal area* (Tokyo: New Energy and Industrial Technology Development Organization), 68p.

Nozawa A 2001 Volcanic sequence of caldera-fill deposits and structure of Okiura caldera, Hakkoda geothermal area, Northeast Japan; *J. Geol. Soc. Japan* **107** 413–431.

Ohba T, Hayashi S and Umeda K 2003 K–Ar ages of volcanic rocks from northern vicinity of Matsukawa geothermal field, Iwate Prefecture; *Bull. Volcanol. Soc. Japan* **48** 367–374.

Ohguchi T, Yoshida T and Okami K 1989 Historical change of the Neogene and Quaternary volcanic field in the Northeast Honshu arc, Japan; *Mem. Geol. Soc. Japan* **32** 431–455.

Ono K, Soya T and Mimura K 1981 *Volcanoes of Japan* (2nd edn). 1: 2,000,000 map series, no. 11 (Tsukuba: Geological Survey of Japan).

Otsuki K 1990 Neogene tectonic stress fields of northeast Honshu arc and implications for plate boundary conditions; *Tectonophys.* **181** 151–164.

Otsuki K, Nakata T and Imaizumi T 1977 Quaternary crustal movements and block model in the southeastern region of the Northeast Japan; *Earth Sci.* **31** 1–14.

Pollitz F F 1986 Pliocene change in Pacific Plate motion; *Nature* **320** 738–741.

Priest G 1990 Volcanic and tectonic evolution of the cascade volcanic arc, Central Oregon; *J. Geophys. Res.* **95** (B12) 19,583–19,599.

Sagiya T, Miyazaki S and Tada T 2000 Continuous GPS arrays and present-day crustal deformation of Japan; *Pure Appl. Geophys.* **157** 2303–2322.

Sakuyama M and Nesbitt R W 1986 Geochemistry of the Quaternary volcanic rocks of the Northeast Japan arc; *J. Volcanol. Geotherm. Res.* **29** 413–450.

Sato H 1994 The relationship between late Cenozoic tectonic events and stress field and basin development in northeast Japan; *J. Geophys. Res.* **99(B11)** 22261–22274.

Smith R L 1979 Ash-flow magmatism; *Geol. Soc. Am. Bull., Spec. Paper* **180** 5–27.

Suzuki T, Eden D, Danhara T and Fujiwara O 2005 Correlation of the Hakkoda-Kokumoto Tephra, a widespread Middle Pleistocene tephra erupted from the Hakkoda Caldera, northeast Japan; *The Island Arc* **14** 666–678.

Taira A 2001 Tectonic evolution of the Japanese island arc system; *Annu. Rev. Earth Planet. Sci.* **29** 109–134.

Tamura Y, Tatsumi Y, Zhao D, Kido Y and Shukuno H 2002 Hot fingers in the mantle wedge: New insights into magma genesis in subduction zones; *Earth Planet. Sci. Lett.* **197** 105–116.

Tsuchiya N, Itoh J I, Seki Y and Iwaya T 1997 *Geology of the Iwagasaki District. Quadrangle Series, Scale 1:50,000* (Tsukuba: Geological Survey of Japan).

Umeda K and Danhara T 2008 Zircon fission-track ages for pyroclastics from the Mutsu-Hiuchidake volcano and the basement rocks, Northeast Japan: Re-examination of the

latest volcanic history; *Japan Mag. Mineral. Petrol. Sci.* **37** 131–136.

Umeda K, Hayashi S, Ban M, Sasaki M, Oba T and Akaishi K 1999 Sequence of volcanism and tectonics during the last 2.0 million years along the volcanic front in Tohoku district, NE Japan; *Bull. Volcanol. Soc. Japan* **44** 233–249.

Valentine G A and Perry F V 2007 Tectonically controlled, time-predictable basaltic volcanism from a lithospheric mantle source (central Basin and Range Province, USA); *Earth Planet. Sci. Lett.* **261** 201–216.

Walker G P L 1980 The Taupo pumice: Product of the most powerful known (ultraplinian) eruption?; *J. Volcanol. Geotherm. Res.* **8** 69–94.

Watanabe T, Koyaguchi T and Seno T 1999 Tectonic stress controls on ascent and emplacement of magmas; *J. Volcanol. Geotherm. Res.* **91** 65–78.

Yamamoto T 2003 Eruptive history of Numazawa volcano, NE Japan: New study of the stratigraphy, eruption ages, and eruption volumes of the products; *Bull. Geol. Surv. Japan* **54** 323–340.

Yamamoto T and Komazawa M 2004 *Geology of the Miyashita District. Quadrangle Series, 1:50,000* (Tsukuba: Geological Survey of Japan).

Yashima R 1990 K–Ar Ages of Pliocene volcanic rocks in Northeast Honshu Arc, Japan: Ajarayama Andesite, Aonokimori Andesite, Nanatsumori Dacite and Sasamoriyama Andesite; *Chikyu Kagaku* **44** 150–153.

Yoshida T 2001 The evolution of arc magmatism in the NE Honshu arc, Japan; *Tohoku Geophys. J.* **36** 131–149.

Yoshida H and Takahashi M 1991 Geology of the eastern part of the Shirakawa pyroclastic flow field; *J. Geol. Soc. Japan* **97** 231–249.

Zhao D, Hasegawa A and Horiuchi S 1992 Tomographic imaging of P and S wave velocity structure beneath Northeastern Japan; *J. Geophys. Res.* **97** (B13) 19,909–19,928.

MS received 7 July 2011; revised 24 July 2012; accepted 25 July 2012